carbon and an overcoat layer. A bare silica singlemode fibre was also monitored as a control.

Measurements have been made in water, at temperatures of between 200 and 300°C and at 4000psi. The unprotected silica fibre shows the effect of the high temperature water where the optical path length increases at 200°C by ~0.45% over 35 days and by a further 0.55% at 250°C over the next 13 days, at which point the fibre failed. The two coated fibres show no signs of path length increase, within experimental uncertainty, at 200 or 250°C over a period of 95 days (note: negative offset of ~-0.01% is attributed to thermal effects of the polymer overcoat layer). On increasing the temperature to 300°C, fibre B changed in path length, but fibre A remained unchanged. However, both fibres failed after only 12 days at 300°C.

On removal of the fibres from the test chamber, it was clear that the failure occurred due to degradation of the carbon coating at small localised regions ~1mm long) along the fibre length. A comparison of the carbon coatings of fibres A and B showed that the former was of superior quality with much fewer damage centres. Whereas the fibre coating failed at 300°C in water after only a very short period, measurements made in polysiloxane oil at 200°C showed no signs of coating damage (to the carbon or the overcoat layer) over a period of 60 days. it should also be noted that most of the world's current oil fields have downhole temperatures of < 200°C.

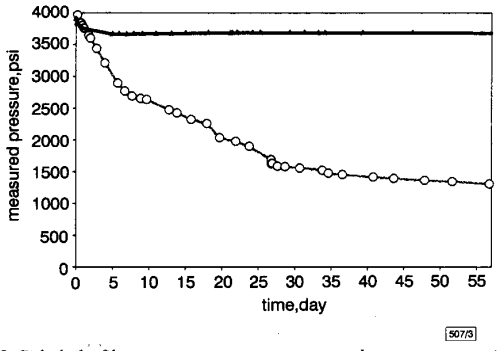

Fig. 3 *Side-hole fibre pressure sensors: measured pressure over time at 155°C and 4000psi in polysiloxane oil*

—○— uncoated silica fibre
—▲— fibre A coated fibre

Fibre optic pressure sensor: Side-hole fibres were coated using the fibre A process and pressure sensors were constructed from these fibres, but without protecung the splice regions. Under hydrostatic pressure, an anisotropic stress and hence a pressure-dependent birefringence is induced in the core due to the side-hole geometry [3, 5]. The pressure sensor used in this investigation consists of an input fibre polariser spliced at 45° to the birefringent axes of a length of side-hole fibre which is terminated by a mirror. The pressure-induced birefringence in the sensor head is remotely monitored using a thermal-scan-matched low-coherence interferometer [6].

Fig. 3 shows stability results of coated and bare silica side-hole fibre pressure sensors monitored in polysiloxane oil at 155°C under 4000psi for ~2 months.

The coatings clearly result in an impressive reduction in drift. Over 57 days the coated sensors showed a 100-fold improvement in drift. Ignoring the first 5 days where the sensor stabilises, the reduction factor is ~ 200 times. In practice, the sensors can be pre-aged and recalibrated to remove the initial change. The total drift (after the period of stabilisation) of the coated sensor is < 5psi over almost 2 months. However, two splice regions of the sensor were not coated. For the sensors used in this experiment (~ 25cm long), almost 1% of the sensor was therefore uncoated. In due course, a coating process will be required to protect the splice regions and further reduce drift.

Conclusions: The cause of drift in silica fibre pressure sensors in fluids at high temperatures has been identified and a solution in the form of hermetic coatings has been tested. A carbon and protective overlayer dual coating has shown substantial improvements. Sensors fabricated using this coated fibre have shown reductions in drift by a factor of 200 in polysiloxane oil at 155°C. The performance of these sensors makes them suitable for use in many of today's hotter oil wells.

13 April 1999
Electronics Letters Online No: 19990646
DOI: 10.1049/el:19990646

J. Clowes, J. Edwards, I. Grudinin, E.L.E. Kluth and M.P. Varnham (*Sensor Dynamics Ltd., Winchester, Hampshire, United Kingdom*)

M.N. Zervas (*ORC, University of Southampton, Southampton, United Kingdom*)

C.M. Crawley and R.L. Kutlik (*Chevron Research & Technology Co., USA*)

J. Clowes: Also with ORC, University of Southampton, Southampton, United Kingdom

References

1 KLUTH, E.L.E.: 'Remotely deployable pressure sensor'. US Patent 5582064, 1996
2 CLOWES, J., MCINNES, J., ZERVAS, M.N., and PAYNE, D.N.: 'Effect of high temperature and pressure on silica optical fiber sensors', *IEEE Photonics Technol. Lett.*, 1998, **10**, (3), pp. 403–405
3 CLOWES, J., SYNGELLAKIS, S., and ZERVAS, M.N.: 'Pressure sensitivity of side-hole optical fiber sensors', *IEEE Photonics Technol. Lett.*, 1998, **10**, (6), pp. 857–859
4 CLOWES, J., SYNGELLAKIS, S., and ZERVAS, M.N.: 'Finite element modelling of optical fibre pressure sensor drifts'. Unpublished
5 XIE, H.M., DABKIEWICZ, P., ULRICH, R., and OKAMOTO, K.: 'Side-hole fiber for fiber-optic pressure sensing', *Opt. Lett.*, 1986, **11**, (5), pp. 333–335
6 XU, M.G., JOHNSON, M., FAHRADIROUSHAN, M., and DAKIN, J.P.: 'Novel polarimetric fibre device for interrogating white-light interferometers', *Electron. Lett.*, 1993, **29**, (4), pp. 378–379

Multiwavelength fibre source by using long period fibre gratings in superfluorescent fibre source

C.D. Su and L.A. Wang

A new technique is presented for realising multiwavelength fibre source by inserting cascaded LPFGs in a conventional double-pass backward superfluorescent fibre source. The output power of each channel is higher than that obtained by spectrum slicing.

Introduction: Wavelength-division multiplexing (WDM) is an important technique for fibre optical communication since the transmission capability can be increased by orders of magnitude. It is always desirable to have a multiwavelength light source in a WDM system. Such light sources include semiconductor laser arrays [1] or multiwavelength fibre sources [2, 3]. Multiwavelength fibre sources have attracted much attention recently due to their all-fibre configuration and relatively easy installation. Fibre Bragg gratings (FBGs) and long period fibre gratings (LPFGs) have been incorporated in multiwavelength fibre sources. For example, five FBGs have been written in an erbium-doped fibre [2], and cascaded LPFGs have been employed in an Er-doped superfluorescent fibre source (SFS) [3]. Note in the latter case that the filter was placed at the output end of the SFS, leading to a marked power loss. In this Letter, we describe a new technique in which cascaded LPFGs are added inside a double-pass backward (DPB) SFS [4] so as to increase the power from the multiwavelength fibre source for each channel with reduced total power loss.

Experiment setup: Fig. 1 shows the setup of a multiwavelength fibre source in a conventional DPB configuration capable of generating equal channel spacing. The DPB configuration is employed since it would provide higher power than the other configurations [4]. The pump power is launched through a WDM into a 15m-long Er-doped fibre from a diode laser operating at 976nm. Another WDM is used to separate the residual pump signal and the forward signal. A fibre mirror, which provides the double-pass

function, is used to reflect the forward signal to the backward direction. The cascaded LPFGs are positioned between the second WDM and the fibre mirror to provide the filtering effect. An isolator with ~60dB isolation is used to prevent the formation of a resonant cavity due to optical feedback from the output endface. The LPFGs are externally written in a hydrogenated dispersion shifted fibre by using a KrF excimer laser. After exposure, a periodic index variation is formed in the core. The LPFGs are controlled to have the same transmission spectra at the same exposure dosage. The periodic index variation causes light to be coupled from the core mode to the cladding mode when the phase matching condition is satisfied [5]. Since the effective refractive indices of the core mode and cladding mode are different, an optical path difference results after the two modes propagate the same distance between the LPFGs. As the cladding mode is coupled back to the core mode by the second LPFG, it will interfere with the original core mode which leads to an interference pattern. The fibre between the second LPFG and the fibre mirror is coiled to avoid other interference. To obtain a high degree of visibility or contrast for the interference pattern, the power of the core and cladding modes should be almost the same. Therefore, the exposure time should be controlled so as to obtain each LPFG with a peak loss of 3dB so that 50% of light is coupled to the cladding and the other 50% remains in the core.

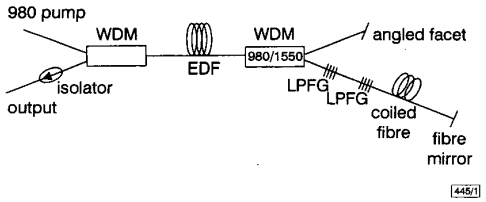

Fig. 1 *Schematic diagram of multiwavelength fibre source*

Results: Fig. 2 shows the transmission spectrum of the cascaded LPFGs. The period of the index variation and the length of the LPFG are chosen to be 400μm and 8mm, respectively, to have a loss band which covers the EDF's gain spectrum. The fibre length between the two LPFGs is controlled to result in a wavelength (channel) spacing of 1.7nm. It is seen that a total of 14 loss peaks in the centre of the LPFG's loss band can have a peak loss > 10dB. The 3dB linewidth of each peak is 0.85nm, half of the spacing.

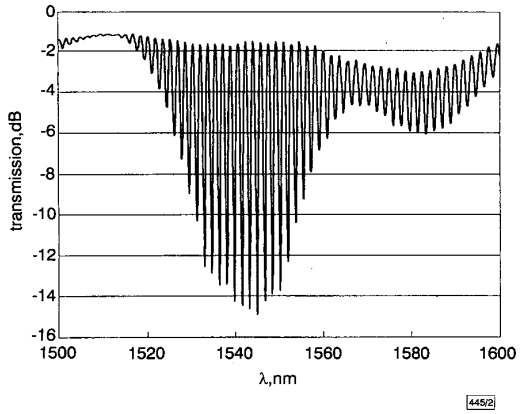

Fig. 2 *Transmission spectrum of cascaded LPFGs*

Fig. 3 shows the output spectra of a multiwavelength fibre source and a spectrum sliced source all based on the same DPB SFS except that the cascaded LPFGs are positioned differently. By inserting the cascaded LPFGs into the DPB SFS, the forward ASE signal filtered by the interference pattern is reflected by the fibre mirror. As the signal passes through the EDF again, the gain is redistributed. The greater the intensity in any spectrum range, the larger the stimulated emission will be in that range. Each peak in the spectrum of the multiwavelength fibre source corresponds to that shown in the interference pattern. Note that the channel spacing of such a source is determined by the distance of two LPFGs. Compared to the spectrum sliced source where the same cascaded LPFGs are placed at the output end, the current configuration of the multiwavelength fibre source allows each channel over the EDF's gain region to have greater output power and higher extinction ratio. Although the cascaded LPFGs introduce an extra loss, the amount is small due to the weak forward ASE signal. The total output power of the original DPB SFS, the multiwavelength fibre source, and the spectrum sliced source are 33.5, 29.5, and 12.8mW, respectively. The power loss of the multiwavelength fibre source is only ~0.55dB, which is smaller than that of the spectrum sliced source, ~4.2dB. Currently only several channels near the centre of the LPFG's loss band have a higher extinction ratio. However, more channels could be obtained by, for example, using LPFGs of shorter length.

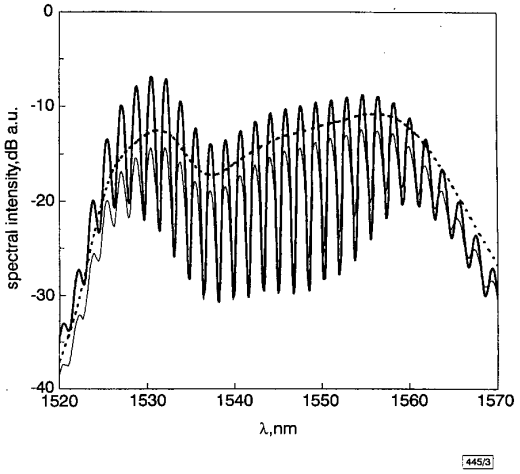

Fig. 3 *Output spectra of multiwavelength fibre source and spectrum sliced source based on a DPB SFS*

multiwavelength fibre source
DPB SFS
spectrum sliced source

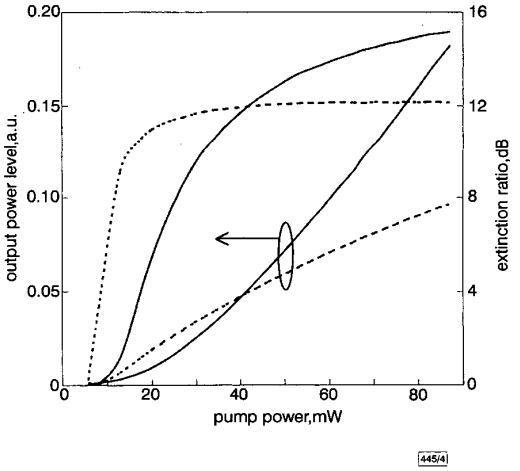

Fig. 4 *Output power and extinction ratio of 1530.4 and 1558.4nm channels against pump power*

1530.4nm
1558.4nm

To study the effect of pump power on the multiwavelength fibre source, two channels centred at 1530.4 and 1558.4nm are selected because these together with all the channels in between have a higher extinction ratio than the rest. As shown in Fig. 4, the output power and extinction ratio of these two channels increase with pump power. If the pump power is not sufficient, little forward signal can reach the fibre mirror, and there is no multiwavelength generation because there is no filtering effect. As the pump power increases, more forward signal is filtered by the cascaded LPFGs, and the extinction ratio increases. The required pump power to

obtain an extinction ratio of > 10dB are 32 and 15mW for 1530.4 and 1558.4nm, respectively, owing to the fact that the absorption coefficient of the EDF is larger at short wavelengths. Additionally, it should be noted that a filter based on self-interference [6] may be used to substitute the cascaded LPFGs for the generation of a high-power multiwavelength fibre source.

Conclusion: We have demonstrated a new method for realising a high-power multiwavelength fibre source by inserting cascaded LPFGs in a DPB SFS. The cascaded LPFGs are positioned before the fibre mirror for gain redistribution so that the multiwavelength fibre source has a larger output power and extinction ratio for each channel, and smaller total power loss compared to the spectrum sliced source with the same LPFGs.

26 February 1999
Electronics Letters Online No: 19990521
DOI: 10.1049/el:19990521

C.D. Su and L.A. Wang (*Institute of Electro-Optical Engineering, National Taiwan University, Taipei, Taiwan, Republic of China*)

L.A. Wang: Corresponding author

E-mail: lon@ccms.ntu.edu.tw

References

1 FARRIES, M.C., CARTER, A.C., JONES, G.G., and BENNION, I.: 'Tunable multiwavelength semiconductor laser with single fibre output', *Electron. Lett.*, 1991, **27**, pp. 1498–1499
2 HUBNER, J., VARMING, P., and KRISTENSEN, M.: 'Five wavelength DFB fibre laser source for WDM systems', *Electron. Lett.*, 1997, **33**, pp. 139–140
3 GU, X.J.: 'Wavelength-division multiplexing fiber filter and light source using cascaded long-period fiber gratings', *Opt. Lett.*, 1998, **23**, pp. 509–510
4 WANG, L.A., and CHEN, C.D.: 'Comparison of efficiency and output power of optimal Er-doped superfluorescent fibre sources in different configurations', *Electron. Lett.*, 1997, **33**, pp. 703–704
5 VENGSARKAR, A.M., LEMAIRE, P.J., JUDKINS, J.B., BHATIA, V., ERDOGAN, T., and SIPE, J.E.: 'Long-period fiber gratings as band-rejection filters', *J. Lightwave Technol.*, 1996, **LT-14**, pp. 58–65
6 LEE, B.H., and NISHII, J.: 'Self-interference of long-period fibre grating and its application as temperature sensor', *Electron. Lett.*, 1998, **34**, pp. 2059–2060

4H-SiC visible blind UV avalanche photodiode

F. Yan, Y. Luo, J.H. Zhao and G.H. Olsen

The first 4H-SiC avalanche photodiode for visible-blind UV applications has been designed and fabricated successfully. The device structure is described and the photo-responsivity characteristics presented. The observation of a positive temperature coefficient for an avalanche breakdown voltage up to 257°C is also discussed.

SiC is an ideal semiconductor for high speed and high gain visible blind UV detectors due to its large ionisation coefficient ratio between holes and electrons (~100) [1]. However, since the critical field for SiC is almost 10 times higher than that of Si, it is very difficult to fabricate SiC *pn* diodes with bulk avalanche breakdown [2]. In this Letter we report the first 4H-SiC avalanche photodiode (APD) fabricated with mesa edge termination, passivated with a high quality thermal oxide. A maximum responsivity as high as 106 A/W, which is > 600 times higher than that of conventional 6H-SiC *pn* photodiodes, has been obtained [3].

A reach-through APD (RAPD) structure with hole initiated impact ionisation has been designed for operation within 100V. The cross-sectional view of the RAPDs is shown in the inset of Fig. 1. A three layer structure grown on n^{++} (> 10^{19}/cm^3) Si face 4H-SiC substrate is used to fabricate the 4H-SiC RAPDs. The top p^{++} layer forms the *pn* junction together with the *n* layer, which also serves as the multiplication region. The *n* layer is the reach-through layer, which absorbs photons and drags photogenerated holes into the multiplication layer. The doping concentrations and the thicknesses from the p^{++} to the *n* are 2.5×10^{19}/cm^3 and 0.15μm, 5.4×10^{17}/cm^3 and 0.4μm, and 3.1×10^{15}/cm^3 and 1μm, respectively. The variation of the *n* layer doping concentration is determined to be within $\pm 0.5 \times 10^{17}$/cm^3 by CV measurement.

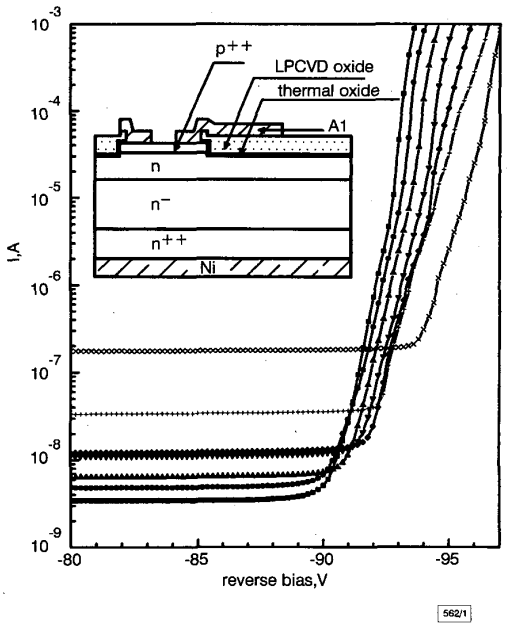

Fig. 1 *I-V characteristics under reverse bias measured at various temperatures*
■ 27°C
● 57°C
▲ 97°C
▼ 130°C
● 173°C
+ 215°C
× 257°C
Inset: cross-sectional view of RAPDs

The fabrication of the RAPD is as follows. A 0.4μm deep mesa is first formed by the inductively coupled plasmas (ICPs) etching to isolate the $p^{++}n$ junction. After that, 1 min *in situ* ICP 'cleaning' is carried out at a substrate DC bias of –50V as described in [4] to improve the surface quality. A 80nm thick high quality thermal oxide is then grown in wet oxygen at 1100°C for 6h followed by 1h *in situ* annealing in ultra-high purity Ar, which resulted in a very low effective charge and interface trap density [5]. Next, 1μm of LPCVD SiO_2 is grown on top of the thermal oxide at 900°C, followed by wet etching to open an oxide window on top of the mesa for a *p*-type Ohmic contact. Finally, Al and Ni are sputtered on the front and back for the *p*-type and *n*-type Ohmic contacts, respectively, and the optical window is opened. Four different sizes of RAPDs are fabricated. The breakdown voltages and their temperature dependent property are found to be independent of the device sizes. The results for RAPDs with a device size of $85 \times 85\mu m^2$ and optical window size of $57 \times 57\mu m^2$ are presented next, which show a peak responsivity of 106A/W.

The DC electrical characteristics of the RAPDs are studied using an HP4145B semiconductor parameter analyser. Their response spectra are measured using a 150W UV enhanced Xe arc lamp, a monochromator with 2400g/mm UV optimised grating, an optical chopper, a UV microscope objective with the spot size smaller than 50μm, an XYZ translator, and a lock-in amplifier in a synchronous detection scheme. The power of the incident light is measured by an Si photodiode detector calibrated from 200nm to 1μm.

Most of the 4H-SiC RAPDs show a positive temperature coefficient for breakdown voltage. No localised or edge related light emission is observed on the RAPDs with a positive temperature coefficient when the RAPDs are driven into avalanche mode. However, when the breakdown current is higher than 100A/cm^2, a very dim grey light is emitted uniformly from the optical window.